Exploring Polarization in Hybrid Modulation for LED-Camera Communication

Xiang Zou, *Student Member, IEEE,* Jianwei Liu, *Student Member, IEEE,* Jinsong Han, *Senior Member, IEEE,* and Zhi Wang

Abstract—With the popularity of LED infrastructure and the camera on smartphone, LED-Camera visible light communication (VLC) has become a realistic and promising technology. However, the existing LED-Camera VLC has limited throughput due to the sampling manner of camera. In this paper, by introducing a polarization dimension, we propose a hybrid modulation scheme with LED and polarization signals to boost throughput. Nevertheless, directly mixing LED and polarized signals may suffer from channel conflict. We exploit well-designed packet structure and Symmetric Return-to-Zero Inverted (SRZI) coding to overcome the conflict. In addition, in the demodulation of hybrid signal, we alleviate the noise of polarization on the LED signals by the polarization background subtraction. We further propose a pixel-free approach to correct the perspective distortion caused by the shift of view angle by adding polarizers around the liquid crystal array. We build a prototype of this hybrid modulation scheme using off-the-shelf optical components. We enhance the basic version [1] of preliminary work by analyzing the performance with FSK modulation. Extensive experimental results demonstrate that the hybrid modulation scheme can achieve reliable communication, achieving 13.4 kbps throughput, which is 400 % of the existing state-of-the-art LED-Camera VLC.

Index Terms—Visible light communication, polarization, hybrid modulation

1 Introduction

Visible light communication (VLC) has received extensive attention and become an alternative to radio frequency communication due to its wide spectrum of advantages, including the large frequency band and channel capacity, as well as high security [2], [3], [4], [5], [6], [7]. However, it is still difficult to implement existing VLC approaches in reality, because of their high requirements on the hardware components, such as the Light Emitting Diodes (LEDs) with high frequency response or the Photo-Diodes (PDs) with high sampling rate [8], [9], [10], [11]. Recently, researchers have set their sights on practical VLC systems that only involve commercial-off-the-shelf (COTS) devices. Benefiting from the widespread deployment of LED luminaires and the proliferation of camera-equipped smartphones, LED-Camera VLC becomes a promising solution. A LED-Camera VLC system usually uses COTS LEDs as the transmitter and camera (widely adopted in portal devices, e.g., smartphones) with rolling-shutter effect as the receiver [1], [12], [13], [14], [15], [16], [17], [18].

Since camera is widely used in commercial devices, LED-Camera communication has created many novel applications. For example, in the shopping mall, the light near the commodity can deliver the advertisements and detailed information of the merchandise [14]. In some scenarios like electronics factory where electromagnetic communication is not allowed, user can communicate by light. In addition, compared with radio frequency communication, visible light communication infrastructure is almost free due to the popularity of indoor LED lights [13]. Meanwhile, the energy consumption of VLC communication is negligible.

However, there seems an impenetrable barrier for current LED-Camera VLC towards high throughput. Due to the sampling manner of rolling shutter, the throughput of LED-Camera VLC is limited to less than 5 kbps. While existing VLC system can send user identification codes or commodity price with low throughput, image enabled advertisement or high-quality conversation require higher throughput. Existing solutions cannot meet the required high throughput. Essentially, the throughput of LED-Camera VLC is constrained by the dimensionality of the data received by the rolling shutter-based camera. In general, the pixels of a single frame of the camera with rolling shutter effect are sequentially sampled column by column. The number of columns is restricted by the effective resolution of the image sensor in the camera. Bit '1'/'0' is modulated by turning ON/OFF the LED in traditional OOK modulation [12], and the bright/dark luminance forms bright/dark bands ('1'/'0') in a frame of camera. Therefore, multiple data-carrying bands can be received in a frame. Since a column of pixels (i.e., a band) can only represent one bit of information, a frame can only carry 'one-dimensional data'. For example, as shown in Fig. 1, if LED modulates data '01010' by turning ON/OFF LED, the receiver can observe bright/dark bands of LED signals.

In this paper, we aim to remarkably increase the throughput of LED-Camera VLC by superposing extra dimensions. The key idea is to utilize polarization for this augmentation.

- *X. Zou is with the School of Computer Science and Technology, Xi'an Jiaotong University, Shaanxi 710049, China. E-mail: Xiang_Zou@stu.xjtu.edu.cn.*
- *J. Liu and J. Han are with the School of Cyber Science and Technology, Zhejiang University, Zhejiang 310007, China. E-mail: jianweiliu, hanjinsong@zju.edu.cn.*
- *Zhi Wang is with the School of Software Engineering, Xi'an Jiaotong University, Shaanxi 710049, China. E-mail: zhiwang@xjtu.edu.cn.*
- *Corresponding author: Zhi Wang.*

Manuscript received April 19, 2005; revised August 26, 2015.

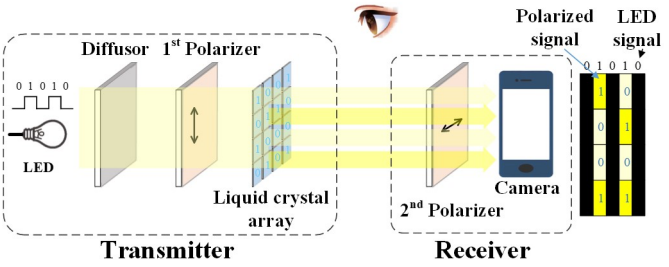

Fig. 1: Illustration of our hybrid modulation design. LED and LC array modulate data together. Human eyes are insensitive to polarized light, while the receiver can obtain LED signals and polarized signals simultaneously by attaching a polarizer in front of camera.

Specifically, we circumvent the data limit in a band of conventional rolling shutter by adding a polarized light array. As illustrated in Fig. 1, we add a polarizer and a liquid crystal (LC) array in front of the light source (i.e., LEDs) to produce polarized light. A diffusor[1] is used to soften the light intensity and produce uniformly polarized light. In this way, the camera can receive multiple bits modulated by polarized light in a band by adding another polarizer film in front of the camera. This hybrid modulation scheme not only preserves conventional LED-Camera channels, but also introduces new polarized channels. Since such a design is inexpensive and convenient to deploy on current LED luminaires [19], [20], we believe that this hybrid scheme will break the limitation of LED-Camera VLC in real implementations.

However, the above solution raises a conflict between the LED signal and polarized signal. That is, during the modulation process, LED will turn off if modulating a bit '0'. In this dark state, polarization modulation cannot be performed. In a nutshell, the LED signal and polarized signal cannot coexist in the dark state. To solve this issue, we propose a novel encoder - Symmetric Return-to-Zero Inverted (SRZI) and a well-designed packet structure according to the response time difference between the LED and LC. The insight behind SRZI is that bright bands appear alternately in two consecutive frames. With this coding strategy, the polarized signal can be recovered by splicing bright bands in these two frames. Eventually, the LED signal and polarized signal can be concurrently transmitted.

In practice, we encounter two challenges in the demodulation. First, since the LED signal is mixed with some noise caused by polarization, the signal-to-noise (SNR) ratio of the LED-Camera channel would be reduced, degrading the demodulation accuracy. Second, unlike the pure-polarized VLC [19], [20], the LC array in our scheme suffers from perspective distortion [21], [22] caused by the variation of view angle. To solve this problem, traditional solutions [23], [24], [25] set extra markers as the positioning assistance, like the three position markers in a QR code [23], which usually occupy certain number of pixels in the corners. However, it is hard to be applied in our scheme because the limited number of pixels in the LC array can hardly afford extra markers.

To tackle the first challenge, we exploit the similarity of polarized signal among multiple frames during the polarization modulation to alleviate the noise in the bright bands. This significantly improves the SNR of LED signals. For the second challenge, we place a piece of polarizer around the LC array on the transmitter's side. The polarizer outlines the boundary of the LC array. In particular, the polarization direction of this polarizer is deliberately set to be different from that of the polarized light. Additionally, a dispersor is used to divert polarized light into different colors. On the receiver's side, we can detect the boundary (including corners) of the LC array according to color difference. This treatment is inspired by our observation on the insensitivity of human eye to the directionality of polarized light [19], [20], [26]. In this way, our scheme achieves the effect of 'corner positioning' in a pixel-free fashion.

We prototype our scheme with COTS devices: a lamp to modulate visible light, a modified 128x64 LC array to create polarized lights, and a smartphone to receive the hybrid signal of light and polarization. We perform extensive experiments and the results show that our scheme can achieve reliable communication with a throughput of 13.4 kbps, which is 400 % of the existing state-of-the-art LED-Camera VLC. In summary, the contributions of this paper are as follows.

- We propose a new hybrid modulation scheme supported the transmission of LED signal and polarized signal concurrently. The proposed scheme utilizes a novel symmetric coding mechanism and packet structure to achieve hybrid signal transmission, breaking the limitation of data dimension in conventional LED-Camera VLC.
- Leveraging the biological fact that humans' eyes are insensitive to the direction of polarized lights, we propose to employ a polarizer to enable corner positioning of perspective distortion image in a pixel-free way.
- We build a prototype of our scheme and conduct extensive experiments. The results demonstrate that our scheme can tremendously boost the throughput of LED-Camera VLC, and its cost-efficient and COTS implementation will facilitate the VLC deployment in practice.

The rest of this paper is organized as follows. We introduce the background of LED-Camera communication and polarized light modulation in Sec. 2. The hybrid modulation scheme is presented in Sec. 3. In Sec. 4, we propose the demodulation method in hybrid signals. We report and discuss the evaluation result in Sec. 5 and Sec. 6. We conclude our paper in Sec. 7.

2 Background and Related Work

In this section, we briefly introduce the rolling shutter effect and polarization modulation. Moreover, we investigate existing LED-Camera and polarization communication approaches in the literature.

1. Diffusor is often used in lighting infrastructure to avoid damage to human eyes caused by high-intensity light emitted by LEDs.

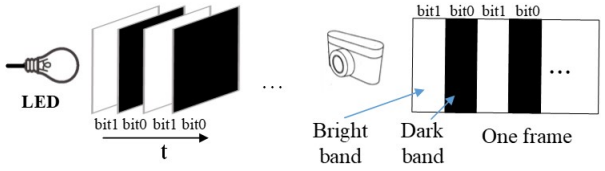

Fig. 2: Rolling shutter effect. The LED transmits data through rapid changes of ON/OFF state, which are captured by rolling shutter-based camera as bright/dark bands.

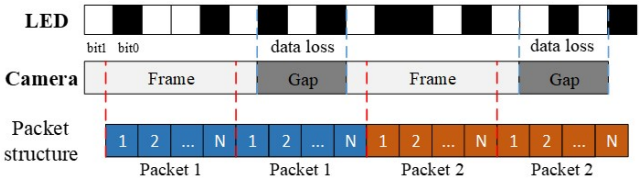

Fig. 3: A repetition packet structure with a gap between two continuous frames.

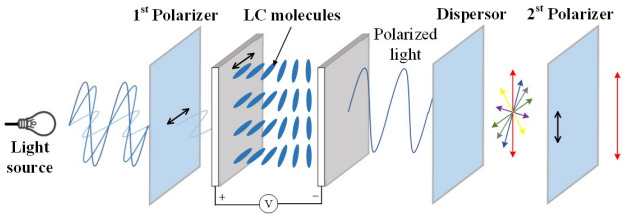

Fig. 4: Illustration of the principle of liquid crystal rotating polarized light. Visible light is converted to polarized light by the first polarizer, which is then rotated by the liquid crystal. The dispersor transfers polarized light into color beams. The second polarizer outlies colors different from polarization direction and retains one color of light beam.

2.1 LED-Camera Communication

Rolling shutter effect is the basic of LED-Camera communication. The rolling shutter-based camera exposes and samples the pixels of a single frame in a column-by-column manner. If using On-Off Keying (OOK) to modulate bit '1'/'0', i.e., turning the LED ON/OFF, a certain number of bright/dark bands in a frame can be captured by the camera, as shown in Fig. 2. By demodulating the captured bands, the receiver can retrieve the transmitted information. In addition, the flicker frequency of VLC should be greater than 200 HZ [2], with the consideration of lighting function of VLC and avoiding visible flicker of data transmission from harming human eyes.

There are two types of LED-Camera communication systems according to whether the influence of the gap [27], [28] between frames is involved or not. As illustrated in Fig. 3 , the data modulated by LED is lost in the frame gap. Traditional LED-Camera communication systems do not take this gap into account and achieve a throughput of 3.1 kbps at a distance of 12 cm by using OOK modulation [12]. The throughput is still lower than 3.2 kbps, even enhancing the LED-Camera communication via high-order modulation (e.g., GSK [17] or CASK [16], which increase the data size carried in each band). To achieve higher throughput, recent researchers adopt colorful LED luminaires for data transmission and improve the throughput to 7.7 kbps [29]. Nevertheless, these colored LEDs cannot be used practicality in commercial lighting infrastructure that usually applies white LEDs.

By involving the aforementioned frame gap, researchers [15], [28] propose to use Frequency-Shift Keying (FSK) to achieve a more robust demodulation scheme, but the throughput is only 11.32 Bps. In addition, IoTorch [27] uses packet repetition in one frame and decodes packets via header detection, enabling a 2.92 kbps throughput. Its packet structure is shown in Fig.3. The frame can capture a complete packet within a repetition mechanism.

Albeit the improvement in the data rate (i.e. throughput), the throughput of existing studies is still limited by the number of bands in the frame. Considering the high-throughput requirement for the VLC system in IEEE standard [2], i.e. minimum data rate required of 11.67 kbps, there is an urgent need to break the data rate limitation of LED-Camera communication.

2.2 Polarized Light Modulation

Recently, the polarized light is utilized for LED-Camera VLC [19], [20], [30]. POLI [20] achieves flicker-free polarized light communication by using multiple LEDs, each LED deploying a polarizer with a different polarization direction, realizing 71 Bps throughput. These systems in [19], [30] employ a single LC cell to modulate data by changing polarized light to different directions. As shown in Fig. 4, the incident light is converted to polarized light by a polarizer. Then, the polarization direction of this polarized light is diverted by the LC cell. If no voltage is applied to the LC, the direction of the incident polarized light will be rotated 90°. The dispersor diverts this light into different color beams with various polarization directions. The second polarizer enables a polarized color beam to pass where the polarization direction of the beam is the same as this polarizer. If a voltage is applied, the polarization direction of the light is rotated with the change of the voltage, thereby changing the polarized color beam. Different colors can be used to represent various information. However, these works can only achieve a throughput of fewer than 1 kbps owing to the limitation of LC response time [31].

In this paper, we break the throughput limit of LED-Camera communication by exploring a new polarization dimension. By adding an LC array, the bright band in a frame can additionally carry polarized signals to increase the overall data rate.

3 Hybrid Modulation Design

We aim at boosting the throughput of LED-Camera communication by introducing a polarization dimension to enable hybrid modulation. For doing so, intuitively, we can simultaneously mix and transmit the LED signal and polarization signal, and then receive them at the camera end. However, there is a conflict between the LED channel and polarization channel when these two kinds of signals are transmitted concurrently. Specifically, since the LC array itself cannot

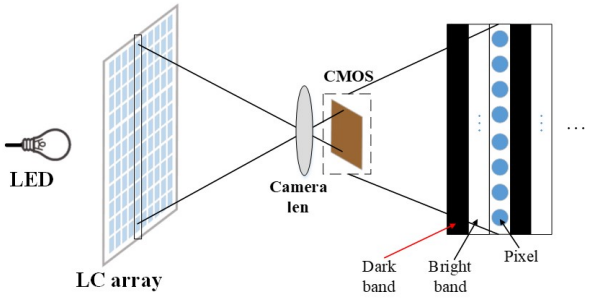

Fig. 5: Illustration of hybrid modulation. The LED and LC array transmit data simultaneously, and CMOS camera receives the hybrid signal. The LED signal is represented by bands, and the bright bands of column pixels contain polarized signals.

emit light, it requires an extra light source to empower its signal transmission. In our hybrid modulation scenario, the LED plays the role of such a light source. However, LED will be turned off when generating a dark band. At this time, due to the 'downtime' of the light source, the polarization signal will be lost.

In this section, we first study the hybrid modulation that can maximize the throughput of the hybrid signals, in which we meet the challenge of channel conflict (Sec. 3.1). Then, in Sec. 3.2, we design a special packet structure based on the response time difference between the LED and LC. With this packet structure, we can well modulate hybrid signal and localize frames with conflict. After that, we overcome the channel conflict by splicing LED packets in adjacent frames with SRZI coding as described in Sec. 3.3. For robustness consideration, we propose packet shift method for FSK modulation as described in Sec. 3.4. Our eventual hybrid modulation scheme is detailed in Sec. 3.5.

3.1 Challenge of Hybrid Modulation

Generally, the frequency response of commercial LED can reach a few MHz [32], and its response time is much less than the sampling period of the rolling shutter camera. Even for the advanced smartphone camera (e.g. Samsung ISOCELL HMX with 12032 $\times$ 9024 pixels [33]), the sampling frequency (10 kHz) is less than the frequency response of LED. Therefore, the relatively low sampling frequency of the rolling shutter camera is the bottleneck limiting the throughput of LED-Camera VLC.

In traditional LED-Camera communication, the intensity of pixels in one column is the sum of optical energy in the exposure duration. These pixels can only represent one bit of information quantified by the intensity. We aim to increase the data rate of LED-Camera communication by introducing a polarization channel, i.e., hybrid modulation with LED and polarization signals. To maximize the throughput gain brought by the introduction of the polarized channel, we want each column to carry as much data as possible. This can be realized by adding a LC array in front of the LED, as shown in Fig. 5. Such a design enables the camera to receive multiple polarized signals in each column, making full use of each column's pixels. This hybrid modulation increases the dimensionality of the data carried by a band on the basis

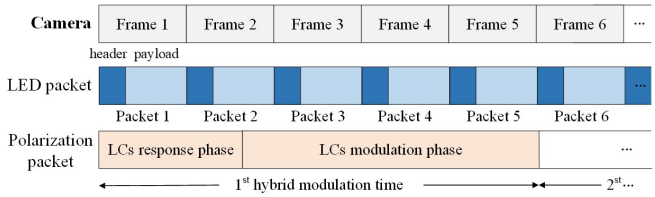

Fig. 6: Structures of LED packet and polarization packet in the hybrid modulation. A LED packet can be carried in a frame, while a polarization packet spans five frames.

of the original LED-Camera communication. Here, we use bit mapping to modulate the polarized signal.

However, the above modulation scheme also induces a conflict between the LED signal and the polarization signal. When the LED modulates bit '0', the LED is turned off, resulting in the absence of the light source for the LC array. The camera cannot receive any polarized signal in the dark band, leading to the loss of information in the polarization channel. To address this challenge, in the following two subsections, we propose a well-designed packet structure and a Symmetric Return-to-Zero Inverted (SRZI) coding strategy. With these two countermeasures, we can recover the lost polarized signals to maximize the benefit brought by the hybrid modulation.

3.2 Packet Structure Design

our goal is to increase the information carried in a frame by modulating both the LED signal and the polarized signal simultaneously. The hybrid signal can be received by the camera. However, as aforementioned, the camera cannot receive complete polarized signals due to the presence of dark bands. Fortunately, we find that there is a large difference between these two kinds of signals in the time domain. More specifically, due to the diversity of hardware, the time spent in modulating the LED signal and polarized signal is different. The frequency response of LED is much higher than the sampling frequency of the camera. In traditional LED-Camera VLC, one frame can take in 100-200 bands of LED signals. The duration of a band is about 0.15 ms [27], while the modulation element of polarized light, i.e. LC, has a response time larger than 10 ms [34], [35]. Therefore, the response time of LC is much longer than that of LED.

Based on such a response time difference, we design a packet structure for the hybrid modulation. The illustration of the packet structure without considering the gap between frames is shown in Fig. 6. The camera takes video and saves it frame by frame. The frame rate for commercial cameras is about 30 frames per second (fps). One LED packet is modulated in a frame, but we use every 5 frames (about 170ms) to modulate one polarization packet. As the time consumption of 5 frames is much larger than the response time of LC, the LC has enough time to modulate the polarized signal. The polarized signals are modulated based on the polarization state of LC cells. The modulation of the traditional LC can be divided into two stages: the response phase and the modulation phase [31]. Since the LC cell cannot accurately express data within the response phase (the direction of the LC molecules changes slowly, and the direction of the

polarized light cannot be immediately twisted by the LC during the response phase), the polarization packet can only be transmitted stably after the LC cell completes the rotation of polarization direction. Therefore, the camera only receives LED signal in the first and second frames. The camera receives the hybrid signal from the third frame to the fifth frame. After that, we only need to recover the complete polarized signal in the third to fifth frames. In this paper, we define that one *hybrid modulation time* is the period of sampling five frames including two frames with LED signals and three ones with hybrid signals. Each LED packet has a header to indicate the beginning of the data transmission, and a payload to carry the data.

3.3 Symmetric Return-to-Zero Inverted Coding

We note that the polarization packet is unchanged from the third frame to the fifth frame. In addition, the hybrid modulation time contains lots of bright bands of the LED signal. To address the problem of packet collision, we propose to splice adjacent frames with bright bands to recover the polarization packet. We first align two LED packets of adjacent frames by using a strict time control of modulation. For example, when the camera has 30 fps, the total duration of the LED packet in one frame can be set to 1/30 seconds[2]. As Case 1 in Fig. 7 illustrates, we can recover the polarization packet by splicing the bright bands in two packets to form an image. For example, the first bit (i.e., the first location) of the third packet is '1', where the LED was turned on to generate a bright band. The bit in the same location (i.e., the first bit also) of the fourth packet is '0', where the LED was turned off to generate a dark band. Since the camera cannot receive the polarized signal in a dark band, we discard the dark band of the fourth packet and take the bright band of the third packet as the first band of the spliced image. For each of the following locations in the two packets, if that of any packet is a bright band, we can choose the bright band to get an image filled with bright bands. In this way, the conflict between the LED signal and the polarized signal in Case 1 is avoided.

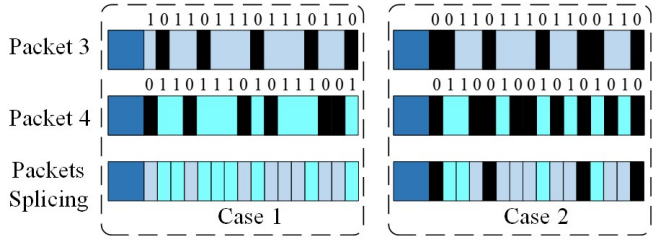

Fig. 7: Bright bands extraction from two packets in adjacent frames of one hybrid modulation time. Case 1: the polarization packet can be successfully recovered with spliced bright bands. Case 2: the polarization packet cannot be recovered when two packets have bit '0' at the same location.

However, if there is a location where both two packets have bit '0', no bright bands can be used to recover polarized signals in this location, as Case 2 shown in Fig. 7. To solve this problem, we propose an encoder - Symmetric Return-to-Zero Inverted (SRZI) coding. As shown in Fig. 8, we first apply 4B6B Run Length Limit (RLL) coding for DC balance and flicker mitigation [2]. The 4B6B coding can eliminate the bit sequences that contain more than three consecutive '1'/'0' by generating 6 encoded bits for every 4 bits (the detail of 4B6B mapping is in Table 4 of [2]). Then, we can perform SRZI coding on the two adjacent packets in Case 2 to eliminate the dark bands. For the third frame, SRZI coding requires bit '1' to be modulated using high amplitude, and bit '0' to be represented using one low amplitude and one high amplitude. As for the fourth frame, bit '0' is modulated with one high amplitude and one low amplitude which is symmetric to the third frame. With this treatment, there is always a high amplitude at any location of two packets with bit '0' as shown by the blue area in Fig. 8. By using SRZI coding, the bright band can always be found in two packets that need to be spliced. Since the coding efficiency of 4B6B is 2/3 [2], we only use 4B6B and SRZI coding for the third frame to the fifth frame. Other frames in the hybrid modulation time can be encoded by more efficient encoders (e.g. GSK [17] or ASK [16]).

Although this coding scheme can effectively avoid chan-

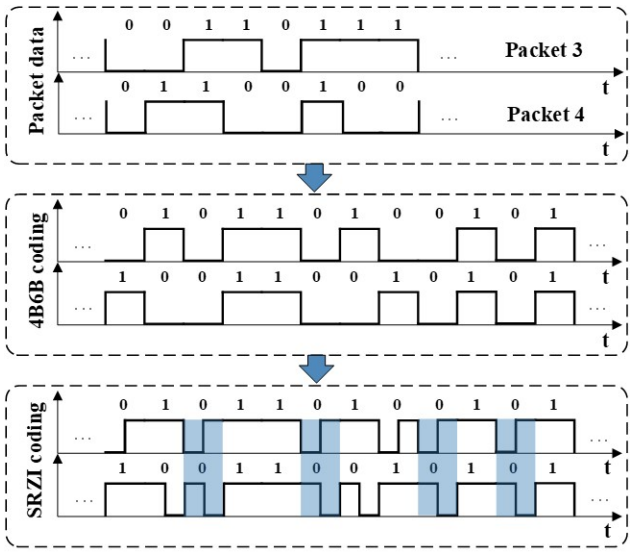

Fig. 8: Two packets are encoded with 4B6B and SRZI. These two packets first apply 4B6B for flicker mitigation, and then are encoded with SRZI for dark band elimination.

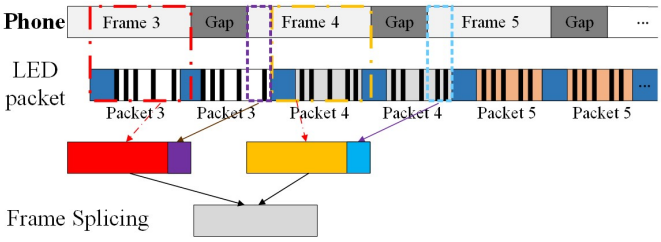

Fig. 9: Combining two parts of packets appeared in three frames to overcome the shift of packet in one hybrid modulation time.

2. The high frequency response of the LED allows us to control the LED signal with high precision to reach microsecond level, so the offset of LED packets is very small.

nel collision, we encounter problems of the packet shift caused by the asynchronization of LED-Camera communication and the gap between two successive frames. The gap will cause the polarized signal not to be fully recovered from one LED packet since the repetition packet structure (as shown in Fig. 3). The packet shift issue will lead to a part of the third packet shift to the fourth frame, as shown in Fig.9. This may cause the packet splicing in the third frame to fail. Similarly, the fifth frame owns the part of the fourth packet. To address this issue, we propose a frame splicing method based on our observation that the length of the packet approximately equals the length of the frame. Particularly, we first calibrate the packet shift. The position at the beginning of the fourth packet is calculated according to the header of the fourth packet, and the part of the third packet in the fourth frame is obtained through image clipping. Since the frame length and packet length are almost equal, the complete third frame containing the third packet can be obtained by splicing the two parts of the third packet. Similarly, the complete fourth frame containing the fourth packet can be obtained by splicing the two parts of the fourth packet, as shown in Fig. 9. Then, the polarized signal can be recovered by splicing the two frames. Note that we need at least three frames to recover the polarized signal due to packet shift.

With above countermeasures, we can overcome packet collision by recovering polarized signals from the spliced image and modulating LED signals with SRZI coding.

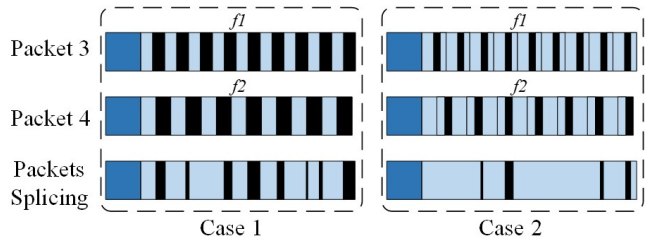

Fig. 10: The polarization packet recovery for FSK. Case 1: the polarization packet cannot be recovered by splicing bright bands of different width. Case 2: the polarization packet cannot be recovered even with SRZI encoding .

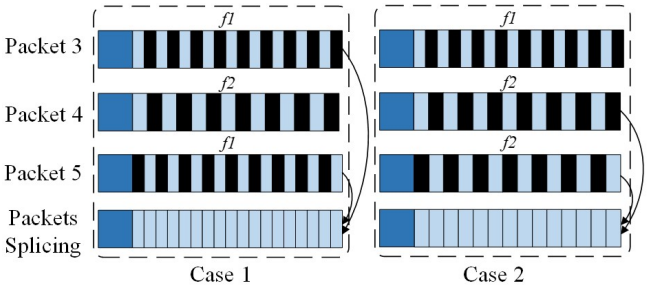

Fig. 11: Bright bands splicing by the shifted fifth packet and a previous packet with the same band frequency. Case 1: the shifted fifth packet is spliced with the third packet of frequency $f1$. Case 2: the shifted fifth packet is spliced with the fourth packet of frequency $f2$.

3.4 Packet Shift for FSK

As aforementioned, we design SRZI coding to address packet collision. However, this coding scheme can only be used when each bit has the same width of band. If we adopt FSK modulation, such a requirement on the width of band cannot be met. Because FSK modulates data with different frequency of bands while the width of band varies with frequency. As a consequence, the polarization packet cannot be recovered by splicing bright bands, as Case 1 in Fig. 10 shows. Even if we use SRZI coding for FSK, the polarization packet still cannot be recovered by splicing bright bands, as Case 2 in Fig. 10 shows. The root cause behind this phenomenon is the unaligned bright bands induced by the differences among band frequency.

To tackle this problem, we leverage the arrangement of bands in FSK to propose a packet shift method to recover the polarization packet. Specifically, the principle of FSK is to modulate the LED with frequency mode and the bands captured by the camera appear to be of a certain frequency. The period of bright or dark bands is equal. In addition, the shift of the band does not change its frequency. Therefore, we perform a shift operation for the fifth packet to recover the polarization packet by alternating the bright bands. As shown in Fig. 11, we shift the fifth packet by half of the period. If the band's frequency of the fifth packet is the same as that of the third packet, the polarization packet can be recovered by splicing the fifth packet and the third packet with frequency $f1$. Similarly, if the band's frequency of the fifth packet is the same as that of the fourth packet, the polarization packet can be recovered by splicing the fifth packet and the fourth packet with frequency $f2$.

Note that the above method can only be applied to Binary FSK (BFSK) [28], that is, this method only works when there are two kinds of band frequency. When a higher-order frequency modulation scheme like 4-FSK is adopted, the band frequency of the fifth packet may be different from that of the third or fourth packet, leading this method to fail. It is worth noting that we can only look for two packets with the same frequency in three successive packets since the valid polarized signal in one hybrid modulation time only contains three packets, as described in Sec. 3.2. In this case, we set the band frequency of the fifth packet as the same as that of the fourth packet. In this way, the polarization packet can be recovered by splicing the shifted fifth packet and the fourth packet.

3.5 Hybrid Modulation Scheme

Fig. 12 shows the block diagram of our hybrid modulation scheme. On the transmitter's side, a header is added to the data at first. Then, the data is segmented into LED packets and polarization packets by calculating the maximum number of bits that the LED and the LC array can hold in one hybrid modulation time. The bits containing the header are assigned to the LED packets and the remaining bits are assigned to the polarization packets. Due to the gap between two continuous frames, the LED packets needs to transmit two identical packets in one frame to avoid data loss in the gap. The conflicting LED packets introduced in Sec. 3.2 are encoded with 4B6B and SRZI coding. Next, the LED packets are modulated using pulse-width modulation (PWM) [27]

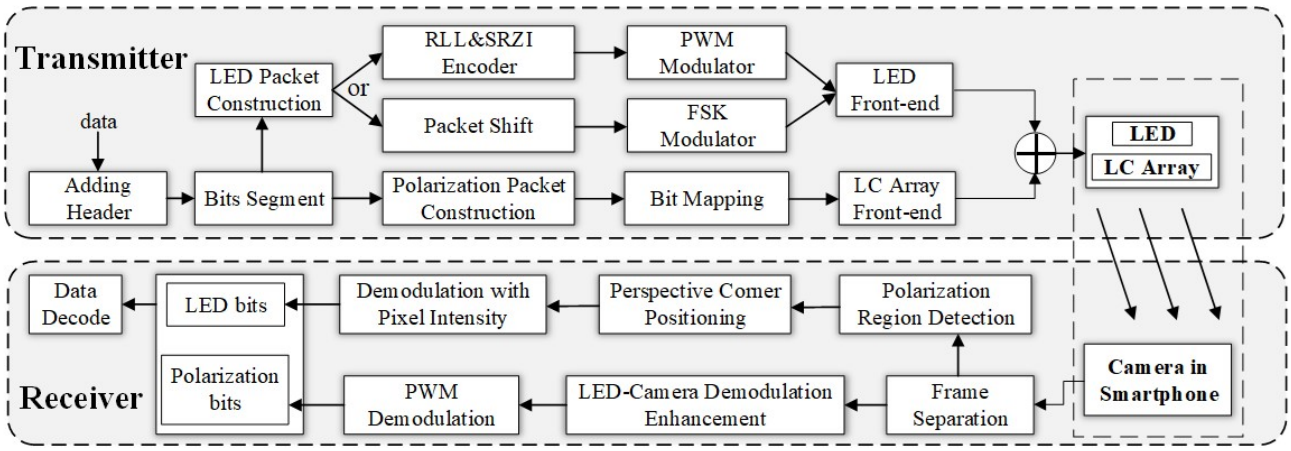

Fig. 12: Block diagram of the hybrid modulation scheme. We introduce a polarization dimension on the basis of LED for boosting the throughput.

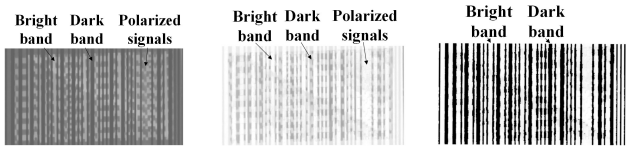

Fig. 13: Noise elimination by subtracting polarization background. (a) The noise of polarized signals in the bright band. (b) The result of noise elimination. (c) LED signal recovered by combining (a) and (b).

and transmitted to the LED front-end. PWM is helpful in optimizing the throughput. In view of the robustness, FSK can also be used to modulate LED signal. In this case, the packet shift operation is performed for the fifth packet in one hybrid modulation time. The polarization packets are transmitted to the LC array front-end by bit mapping. Here, we use four LC cells to modulate one bit. After the above process, the data will be transmitted through modulated light.

4 Demodulation with Hybrid Signals

After the camera receives hybrid signals, we first perform frame separation to obtain frames containing LED packets and the splicing image carrying polarization packets, as shown in Fig. 12. Then, a LED signal enhancement method is used to eliminate the noise of polarized signals. We will detail this method in Sec. 4.1. We demodulate LED signals by rising edge detection [27]. For the image carrying polarized signals, we first perform polarization region detection (Sec. 4.2). Then, the corners of the LC array are determined by our proposed corner positioning method (Sec. 4.3). We detect the header of polarized signal by changing the width of the polarizer (Sec. 4.4). Finally, the polarized signals are demodulated based on the pixel intensity (Sec. 4.5). The data will be decoded by combining LED and polarization bits.

4.1 LED Signal Enhancement

In the hybrid modulation, the LED signals are affected by polarized signals. Typically, the bright/dark bands of LED signals are demodulated by rising edge detection or polynomial fitting [12], requiring bands to have high SNR[3]. However, polarized signals in bright bands decrease the SNR of the LED signal, which reduces the demodulation accuracy. Specifically, polarized light uses the polarization state to modulate data. When the LC cell applies a voltage, the second polarizer blocks the polarized light. Such a block increases the noise of the bright bands. Furthermore, the noise varies with different bright bands. As shown in Fig. 13(a), the SNR of bright bands carrying polarized signals is 0.18. These bright bands with low SNR greatly hinder the demodulation accuracy.

To deal with the above-mentioned problem, we propose to use polarization background subtraction to increase the SNR. Thanks to our designed special packet structure, in each hybrid modulation time containing five frames, the polarized signals do not vary with the frames. We take the splicing image described in Sec. 3.3 as the background of these five frames. The noise of polarized signals on bright bands is eliminated by subtracting the polarization background. In this way, we get bright bands with high SNR of 0.97, as shown in Fig. 13(b). Finally, we extract dark bands in Fig. 13(a) to obtain enhanced LED signals, as shown in Fig. 13(c). Then, we can demodulate LED signals with rising edge detection [27].

However, the polarization state of a LC in the response phase is different from that in the modulation phase. The polarization background in the modulation phase is not exactly the same as that in the response phase. To alleviate the polarization noise of the frames within the response phase of the LC (e.g., the first and second frames), we compare two polarization backgrounds, in which one is the previous splicing image and the other is the present splicing image. After respectively subtracting the first frame to these two splicing images, we take the differences with less noise as the final result.

3. SNR is calculated by dividing the mean of the bright bands by the white pixel value of 255.

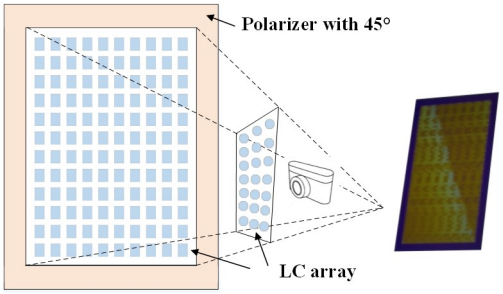

Fig. 14: Perspective distortion due to the shift of view angle. A polarizer is attached around the LC array to detect the polarized signal region.

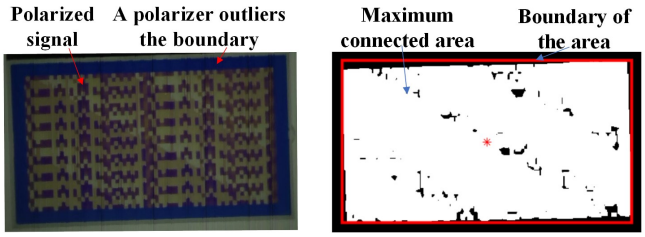

(a) (b)

Fig. 15: The region of the LC array is outlined by a polarizer. (a) The raw image of polarized signals with a special color around LC array. (b) The rectangle boundary around the LC array is determined by using region measurement.

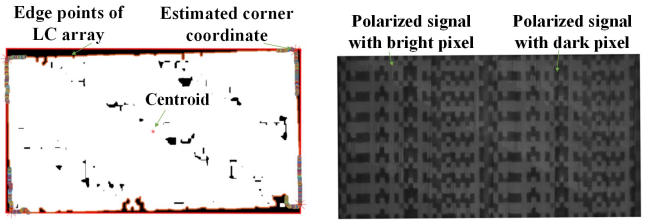

(a) (b)

Fig. 16: The distortion image is corrected with corner coordinates. (a) Four corner coordinates are estimated by calculating the maximum distance from the centroid to edge points of LC array. (b) The final corrected image of polarized signals.

4.2 Region Detection of LC Array

The polarized signal can be demodulated with the splicing image as described in Sec. 3.3. However, the shift of view angle of camera may cause the problem of perspective distortion [21], [22] of LC array, resulting in the shift of the splicing image. As shown in Fig. 14, the shape of the LC array may be distorted when the camera receives polarized signals from an angle.

Traditional camera-based communication requires extra pixels inside the pixel array to form positioning markers. For example, the valid region in QR code can be detected by adding positioning markers at three corners [23] or the centre with color pixels [24], [25]. However, all of these region detection methods require the use of internal pixels to form positioning markers, which is hard to be applied for data modulation in LC array with limited pixel resource. To address this challenge, we propose a pixel-free positioning approach. We take advantage of hybrid modulation to extend positioning markers to the periphery of the LC array without sacrificing LC cells. Specifically, we attach a polarizer that intersects the polarization direction of polarized signal with 45° around the LC array, as shown in Fig. 14. Moreover, inspired by [19], we add a dispersor in front of the array to differentiate the polarization direction of this polarizer. The dispersor is able to convert the polarized light in different directions into different colors. Building on this, we are able to observe a special color around the LC array that is different from the color of polarized signals. The LC array region can be detected by identifying this special color shown in Fig. 15(a). To be specific, we first convert the splicing image to the YCbCr color space [36], highlighting the boundary of LC array. Next, the maximum connected area of the image, which is the region of the LC array, is captured by using region measurement [37], as shown in Fig. 15(b).

4.3 Corner Positioning

Perspective correction requires knowing the corner coordinates of the region [21], [38], [39]. To this end, we first filter out the image noise caused by edge blur. We use the dilation and erosion operation in the field of morphological image processing for filtering. Here, we apply the square structuring element for morphological operation. Then, we extract the edge points of the LC array, as shown in Fig. 16(a). The coordinates of these edge points are easy to be calculated from the binarized image by using region boundary tracing algorithm [40]. Finally, we can obtain four corner coordinates according to the largest distance from the centroid to edge points, as shown in Fig. 16(a). The LC array can be corrected by using perspective correction algorithm described in [39], as shown in Fig. 16(b).

4.4 Header Detection of Polarized Signal

In order to demodulate the polarized signal, we first need to know the start and end of the data. But the image changes as the camera rotates, confusing the location of the start pixel. Straightforwardly, we can adopt the method used in LED signal demodulation to solve this problem, i.e., finding out the start of the valid data by adding and detecting a packet header. Nevertheless, adding a packet header would waste the pixels of the LC array. Thus, we take advantage of the boundary around the LC array described in Sec. 4.2, and propose a packet header detection method based on the centroid of the image. This method does not sacrifice any pixels of the LC array. Specifically, we change the width of the lower polarizer to shift the centroid of the detection region, as shown in Fig. 17. We convert the black pixels around LC array into white ones, so that the region measurement algorithm can capture the outer boundary of the region. The width of the upper polarizer and the lower one can be denoted as $d1$ and $d2$, respectively. If $d1 < d2$, the centroid of the outer region is below the centroid of the inner region, as shown in Fig. 17(b). In this case, We consider

the start pixel of the polarization data to be located in the upper left corner; otherwise, in the lower right corner.

(a) (b)

Fig. 17: The header of polarization data is detected based on the centroid of the image. (a) The different width of upper and lower polarizer. (b) The different centroid of outer and inner region.

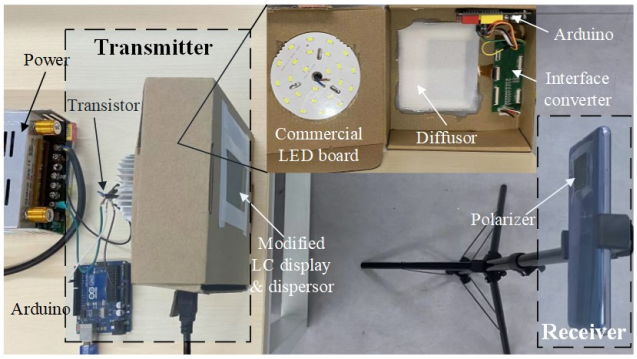

Fig. 18: Experiment setup. The transmitter includes a commercial LED board to modulate LED signals and a modified LC display to modulate polarized signals. The receiver is a smartphone attached to a polarizer.

4.5 Demodulation with Pixel Intensity

The final step is to demodulate the polarization packets using the corrected image shown in Fig. 16(b). First, we mesh the image based on the regular arrangement of the LC array. The number of grid cells is equal to the number of bits in a polarization packet, and the size of the grid cell can be calculated from the number of cells. Then, grid cells are divided into groups. Each group contains eight cells and represents one byte of polarization packet. We perform binary processing on each group and calculate the proportion of black pixels in every cell. For each cell, if the number of black pixels exceeds half of the number of all pixels, it is considered to represent bit '0'; otherwise the cell is represented as bit '1'. With the above process, we are able to correctly demodulate LED signals and polarized signals from hybrid signals.

5 Evaluation

In this section, we evaluate the performance of the hybrid modulation in real scenarios.

5.1 Experiment Settings

Fig. 18 shows the testbed setting of our hybrid modulation scheme for following experiments. We build the transmitter with a commercial LED board and a modified LC display that is inexpensive [19] and easy to deploy. We adopt Arduino UNO as microcontroller and FQPF12N60C transistor ($ 0.3) to drive the COTS illumination LED board (voltage: 40 V, current: 0.3 A, diameter: 85 mm, $ 1.5). A diffusor is placed in front of the LED.

We use a modified commercial LCD with pixel resource of 128×64 to modulate the polarized signal. Commercial LCD is composed of a backlight module, two polarizers, multiple liquid crystal cells, a dispersor and two glass substrates. We remove the backlight module and the upper polarizer from LCD. The LCD is driven by an Arduino UNO. The raw character data is first converted to sexadecimal through ASCII code, and then converted to binary. A character is represented by eight bits, and four LC cells modulate one bit. Moreover, we place a polarizer around the LC array with 45° against polarized light for corner positioning. The dispersor is attached to the LCD to highlight the polarizer. The distance between LED board and LC array is 5cm. The data is segmented in a Raspberry Pi and distributed to LED and LC.

A commercial smartphone HUAWEI Mate 30 is used as the receiver. We set the exposure time to $1/8000$ seconds and the frame rate as 30 fps. The resolution of camera is 1920 $\times$ 1080. We use auto-focus of camera introduced in [28]. A polarizer is attached to the camera [19], [20].

Each LED packet in a frame contains a header with 2 bits and a payload with 5 bytes. Note that, the last three frames in one hybrid modulation time (5 frames) use 4B6B coding which has $2/3$ coding efficiency. Every 5 frames in a hybrid modulation time have 20 bytes of LED packets. The polarization packet is composed of 256 bytes. Every four pixels of the LC display represent a bit. A 128 $\times$ 64 LC display contains 256 bytes. In summary, 276 bytes can be carried in 5 frames. We capture 10 sessions in the following experiments, and each session contains packets with 300 frames. We evaluate the performance of the hybrid modulation scheme with Packet Error Rate (PER) [41], Symbol Error Rate (SER) [27] and throughput with maximum, minimum and average values. The PER is applied for LED signal evaluation and the SER is used for polarized signal evaluation. All experiments are performed in an office environment with ambient light of 420 lux.

5.2 Impact of LED Parameter on Polarization

In this section, we study the performance of polarization communication with different experiment settings of LED.

Width of band. As described in Sec.3.3, the polarized signal is recovered by splicing two LED packets adapting SRZI coding. The width of the LED band in these packets may impact the result of splicing image. To vary the width of bands, we adjust the payload in the LED packet with different bit numbers. The width of band can be expressed as $W_b = W_p/(P + H)$, where W_p is the length of a single LED packet, P and H are the bit numbers in the payload and the header, respectively. We vary the bit number from 48 to 16. The bit number of the relatively long payload is consistent with that described in [27]. Although it is able to set shorter payload, this will significantly reduce

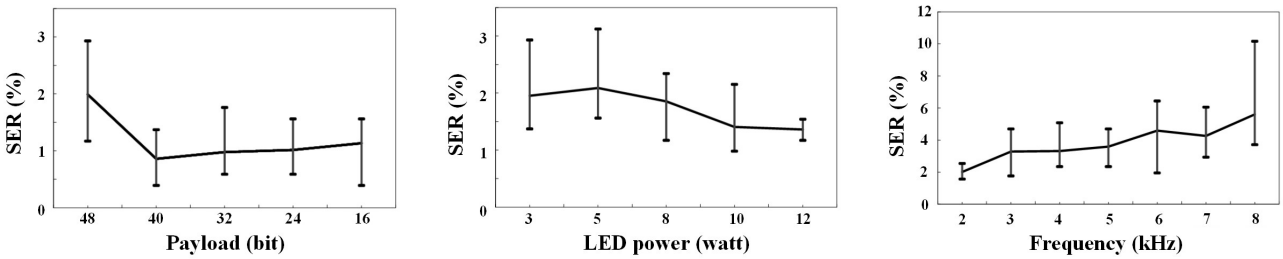

(a) SER vs. Payload. (b) SER vs. LED power. (c) SER vs. LED frequency.

Fig. 19: SER of the polarized signal under different LED parameters. (a) SER varies with bit number in payload of LED packet. (b) SER varies with LED power. (b) SER varies with LED frequency.

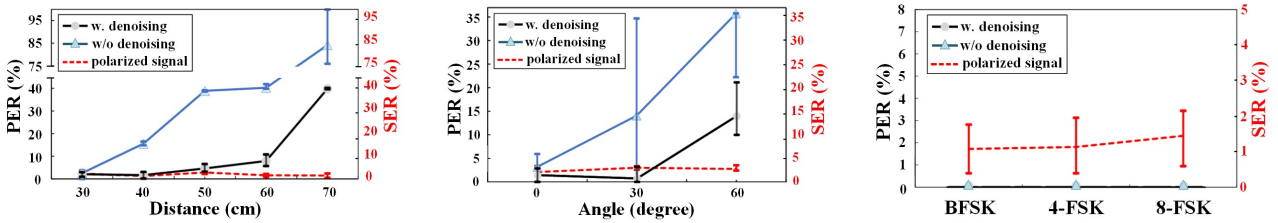

(a) PER and SER vs. Distance. (b) PER and SER vs. Angle. (c) PER and SER vs. FSK.

Fig. 20: PER and SER of hybrid modulation under different experiment settings. (a) PER and SER varies with distance between LED and camera. (b) PER and SER varies with view angle. (c) PER and SER varies with different modulation order of FSK.

the data rate of the LED signal. We calculate the average, maximum and minimum value of the SER in 10 sessions. Figure. 19(a) reports the SER of the received polarized signal under various bit numbers in payload. We can see that the polarized signal has a lower SER when the bit number of payload is less than 40 bits. In the following, we fix the payload of 40 bits.

Power of LED. Another factor that may affect polarization communication is the power of the LED. The polarized signal transmission is empowered by the light of the LED. Low luminance of LED will result in weak polarized signal strength, which may increase SER. Thus, we vary the LED power from 3 to 12 watts. The SER results of the polarized signal are shown in Fig. 19(b). The SER becomes lower as the LED power increases. Overall, the SER decreases insignificantly. We set the LED power to 12 watts in the following experiments.

Frequency of bands. The frequency of bands in FSK may impact the performance of polarized signal recovery. A higher frequency can reduce the band period, thus reducing the precision of packet shift and may affect the recovery effectiveness of polarized signal. In this experiment, we refer to the frequency setting of the literature [28], varying the frequency from 2k to 8k in step of 1k. The SER results of the polarized signal are shown in Fig. 19(c). As expected, the SER becomes higher as the frequency increases.

5.3 Channel Property under Hybrid Modulation

We study the channel property of LED signal and polarized signal under hybrid modulation in this section.

Distance. We change the distance between the LED and the smartphone camera from 30 cm to 70 cm. Figure. 20(a) reports PER and SER of LED signals and polarized signals with the increase of distance. The PER of the LED signal is significantly reduced by denoising the signal as described in Sec. 4.1. In addition, the performance of LED communication degrades with increasing distance. However, the performance of polarization communication remains almost unchanged. The reason behind is that the ambient light reduces the SNR of LED signal with the increase of distance while the polarized signal is almost unaffected by ambient light due to the function of auto-focus and optical zoom of the camera.

View angle. By fixing the communication distance to 30 cm, we examine PER and SER by varying the view angle of camera from 0 to 60 degrees. We define the angle of the camera directly in front of the LED to be 0 degrees. As shown in Fig. 20(b), the change in view angle degrades the performance of the LED communication, while the SER of polarized signal remains almost unchanged. This is because we correct the perspective distortion caused by the shift of view angle of camera in Sec. 4.3. A larger view angle (e.g. 60 degrees) may exceed the irradiance angle of the LED [42], resulting in lower light intensity which leads high PER of LED signal.

FSK modulation. We also evaluate the performance with FSK modulation. We set the distance and angle between the LED and camera to 30 cm and 0 degrees, respectively. BFSK, 4-FSK and 8-FSK are performed to evaluate PER and SER. We set the frequency of bands to 2kHz and 3kHz with BFSK modulation. For 4-FSK, we vary the frequency from 2kHz to 3.5kHz in step of 0.5kHz. For 8-FSK, we vary the frequency from 2kHz to 5.5kHz in step of 0.5kHz. The results are shown in Fig 20(c). It can be seen that the PER of the FSK modulation is zero even without the denoising algorithm. However, the SER of the polarized signal would

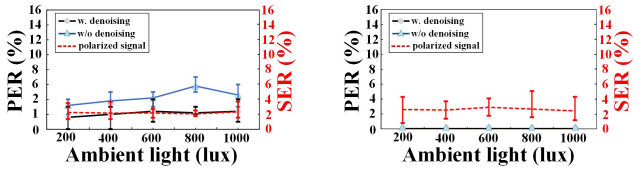

(a) (b)

Fig. 21: PER and SER of hybrid modulation under different ambient light intensity. (a) PER and SER under various ambient light with PWM modulation. (b) PER and SER under various ambient light with FSK modulation.

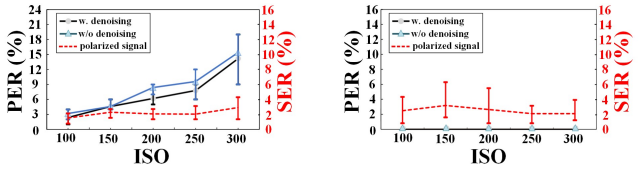

(a) (b)

Fig. 22: PER and SER of hybrid modulation under different ISO. (a) PER and SER under various ISO with PWM modulation. (b) PER and SER under various ISO with FSK modulation.

slightly increase with the increase of the FSK modulation order. This is because higher-order FSK needs to use higher frequency to carry information, and the SER increases with the frequency, as shown in Fig 19(c).

5.4 Performance under Ambient Light

Ambient lights, such as sunlight and other illuminations not used for communication, may affect the performance of hybrid communication. Hence, we investigate the effect of ambient light on communication performance by introducing an additional lighting luminaire. We adjust the ambient light intensity by changing the distance between the luminaire and the receiver. The intensity of the ambient light is measured by a light intensity meter of smartphone [43] at the receiver end. To evaluate the performance of hybrid modulation under different ambient light intensities, we vary the illuminance of ambient light from 200 lux to 1000 lux in step of 200 lux. Fig. 21(a) and Fig. 21(b) show the PER and SER of hybrid signal modulated with PWM and BFSK, respectively. Obviously, the PER and SER of hybrid signals are almost unchanged with the increase of ambient light. The reason behind this is that we use the optical zoom function of camera to zoom in the filming range to the region where hybrid signals exist. This greatly reduces the influence of ambient light on the hybrid signals.

5.5 Impact of ISO on Demodulation

ISO here means the light sensitivity of the camera, which measures how sensitive the film is to the light. ISO directly affects the brightness of the bands at the receiver end. Smaller ISO causes lower brightness of bright bands, yet larger ISO brings more image noise. Fig. 22 reports the experimental results. It can be found that increasing the ISO degrades the demodulation performance of the LED

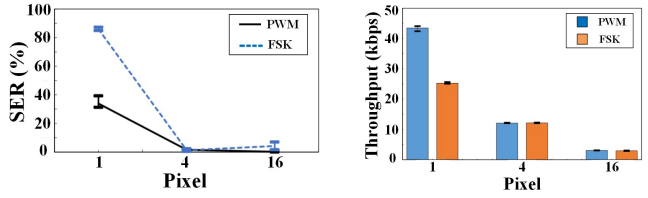

(a) (b)

Fig. 23: SER and throughput of polarized signal under different LC size. (a) SER under various LC size with PWM and FSK modulation. (b) Throughput under various LC size with PWM and FSK modulation.

signal modulated with PWM. This is because the image noise brings blurred boundary between adjacent bands. In addition, the demodulation performance of FSK is not significantly reduced. This is because we only need to know the frequency of bands, rather than the band spacing, for signal demodulation. Moreover, the SER of polarized signal is stable since the image blur brought by a small increase in ISO (like 300) is tolerable for polarized signal. The LED signal modulated with PWM can still maintain high demodulation performance when ISO is lower than 150. Therefore, the ISO can be set to 100 by default.

5.6 Effect of LC Size

In this part, we evaluate the influence of LC size on the performance of polatized signal demodulation. We aim to review a phenomenon that a larger LC size has higher demodulation accuracy but lower throughput [19], i.e., there is a trade-off between LC size and throughput. We use one pixel, four pixels, and sixteen pixels to represent a bit to describe the size of LC, respectively. As shown in Fig. 23(a), the SER significantly decreases with the increase of the LC size. When the LC size is one pixel, the SER even reaches 80 %. The SER is lower than 5 % when the LC size is larger than four pixels. The throughput of the polarized signal is shown in Fig. 23(b). It can be seen that decreasing LC size can significantly increase the throughput, but it would also increase the SER. In consideration of the trade-off, we use four pixels to represent one bit.

5.7 Throughput Evaluations

We evaluate the throughput of the hybrid modulation at different distances and view angles in this section. Moreover, the throughput performance of FSK is studied. We average the data rate every 300 frames to get a throughput of 10 sections. The denoised LED signal is used in this section.

Distance. As in the study of transmission distance in Sec. 5.3, the data rate of LED signal is influenced by distance, while the polarized signal is not. As shown in Fig. 24(a), the throughput of the LED signal decreases with an increasing distance, while the throughput of the polarized signal does not change substantially. The throughput of polarized signal (tens of kbps) significantly improves the overall data rate. In general, the average throughput of hybrid signal is 13.2 kbps, and the maximum throughput can up to 13.45 kbps.

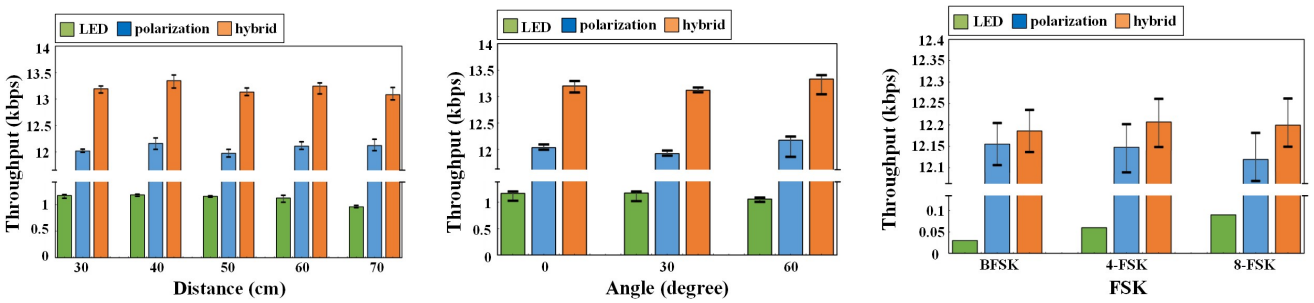

(a) Throughput vs. Distance. (b) Throughput vs. Angle. (c) Throughput vs. FSK.

Fig. 24: Throughput of hybrid modulation under various experiment settings. (a) Throughput varies with distance between LED and camera. (b) Throughput varies with view angle. (c) Throughput varies with different order FSK.

View angle. We then assess the throughput with different view angles of camera. Fig. 24(b) shows the throughput of different view angles. The data rate of polarized signal is still stable rather than LED signal with the change of view angle. The hybrid signal can reach an average throughput up to 13.3 kbps (with a maximum value of 13.4 kbps). This throughput satisfies the requirement of minimum data rate (11.67 kbps) in the IEEE standard for VLC [2]. All results demonstrate the robustness of hybrid modulation in real-world scenarios.

FSK. We also evaluate the throughput of the hybrid signal with FSK modulation of BFSK, 4-FSK and 8-FSK. Fig. 24(c) shows the throughput of different modulation orders of FSK. Apparently, the data rate of LED signal modulated by FSK increases with the increase of the FSK modulation order. Meanwhile, the data rate of polarized signal is still stable. The average throughput of hybrid signal is 12 kbps while the maximum data rate of 8-FSK is 90 bps. Albeit the relatively low data rate, FSK modulation has outstanding robustness.

6 Discussion

Our hybrid modulation scheme has a great security advantage and potential for throughput expansion. Benefiting from the additional polarization dimension, it provides a new direction for increasing the data rate of LED-Camera VLC. As for the reliability issue caused the mobility of the camera, a lot of existing works [21], [24] can be applied to our communication scenario to improve the communication robustness.

Security analysis. VLC has always been considered to be more secure [2], [4], [44] than radio frequency (RF) communication due to its limited communication range. However, recent work [45] shows that VLC is at risk of data leakage through the RF side channel in the non-line-of-sight (NLOS) region, mainly due to the high current (large than 20 mA) and voltage of the wire connecting to the LED. The data of VLC is recovered by sniffing the change of magnetic field caused by the LED wire. By contrast with LED, polarized signal is modulated with LC which is driven by low level voltage (less than 5 V) and small current (less than 1 mA). Therefore, polarized signals reinforce the security of VLC.

Area of the LC array. In this paper, we only explore fixed-area LC array to modulate polarized light, and the number of LC cells is constant (128 $\times$ 64 LC display). The throughput of polarized signal increases linearly with the number of LC cells [19]. Therefore, it is entirely possible to use a larger LC array with more number of LC cells to achieve a higher data rate, which may actually drive the hybrid modulation scheme to achieve Mbps-level throughput.

Overhead. We only use commercial equipment for the testbed. The overhead is very low. The diffusor and polarizer cost \$2 and \$7 respectively. The price of LCD is \$3. Each Arduino for LED and LCD drivers costs \$7. Thus, the hardware overhead caused by the polarized signal modulation is only about \$17. In addition, the modified LCD can be deployed on the lampshade of commercial luminaire. Most lampshades use diffusor for spreading the range of lighting. Our design also requires LC to be deployed on the surface of the diffusor as the light source of the polarized signal. Therefore, LC is very easy to deploy in commercial luminaires.

7 Conclusion

Aiming to break the limit of data rate in LED-Camera VLC, we propose to use polarization dimension to enlarge the amount of data carried in frames. A hybrid modulation scheme is designed to enable hybrid signal transmission of LED and polarization. The scheme is implemented with COTS devices and achieves reliable communication with a throughput up to 13.4 kbps. The key idea is to increase the amount of data in frames by using polarized signals. In addition, to handle channel conflict between LED signal and polarized signal, we design a packet structure of hybrid modulation and propose a SRZI coding to overcome the conflict. We also develop a corner positioning method with a pixel-free way to correct the perspective distortion caused by shift of view angle. We demonstrate the reliable and promising performance of our hybrid modulation scheme through extensive experiments.

Acknowledgments

This work was supported by the National Key Research and Development Project (2022YFB3305503), NSFC Grant No. 62176205 and 62072367, Key Science and Technology Project of Henan Province (201300210400), and Key Research and Development Program of Shaanxi Province (2023-YBGY-403).

REFERENCES

[1] X. Zou, J. Liu, and J. Han, "Breaking the throughput limit of led-camera communication via superposed polarization," in *Proceedings of the IEEE Annual International Conference on Computer Communications, INFOCOM*, 2023.

[2] S. Rajagopal, R. D. Roberts, and S. Lim, "IEEE 802.15.7 visible light communication: modulation schemes and dimming support," *IEEE Communications Magazine*, vol. 50, no. 3, pp. 72–82, 2012.

[3] S. Cho, G. Chen, and J. P. Coon, "Enhancing security in VLC systems through beamforming," in *Proceedings of the IEEE Global Communications Conference, GLOBECOM*, 2020.

[4] G. Blinowski, "Security issues in visible light communication systems," *IFAC-PapersOnLine*, vol. 48, no. 4, pp. 234–239, 2015.

[5] P. H. Pathak, X. Feng, P. Hu, and P. Mohapatra, "Visible light communication, networking, and sensing: A survey, potential and challenges," *IEEE Communications Surveys & Tutorials*, vol. 17, no. 4, pp. 2047–2077, 2015.

[6] A. Jovicic, J. Li, and T. Richardson, "Visible light communication: opportunities, challenges and the path to market," *IEEE Communications Magazine*, vol. 51, no. 12, pp. 26–32, 2013.

[7] M. Cui, Q. Wang, and J. Xiong, "Breaking the limitations of visible light communication through its side channel," in *Proceedings of the ACM Conference on Embedded Networked Sensor Systems, SenSys*, 2020.

[8] R. Bian, I. Tavakkolnia, and H. Haas, "10.2 gb/s visible light communication with off-the-shelf leds," in *Proceedings of the European Conference on Optical Communication, ECOC*, 2018.

[9] Z. Yu, C. Gong, J. Wei, N. Huang, and Z. Xu, "3-gb/s visible light communication over 5 m distance based on imaging system with low transmission power and off-the-shelf leds," in *Proceedings of the International Wireless Communications and Mobile Computing, IWCMC*, 2021.

[10] C. Lin, Y. Yu, J. Xiong, Y. Zhang, L. Wang, G. Wu, and Z. Luo, "Shrimp: a robust underwater visible light communication system," in *Proceedings of the Annual International Conference on Mobile Computing and Networking, MobiCom*, 2021.

[11] H. Wu, Q. Wang, J. Xiong, and M. Zuniga, "Smartvlc: Co-designing smart lighting and communication for visible light networks," *IEEE Transactions on Mobile Computing*, vol. 19, no. 8, pp. 1956–1970, 2020.

[12] C. Danakis, M. Z. Afgani, G. Povey, I. Underwood, and H. Haas, "Using a CMOS camera sensor for visible light communication," in *Proceedings of the IEEE Workshops of the Global Communications Conference, GLOBECOM*, 2012.

[13] J. Hao, Y. Yang, and J. Luo, "Ceilingcast: Energy efficient and location-bound broadcast through led-camera communication," in *Proceedings of the IEEE Annual International Conference on Computer Communications, INFOCOM*, 2016.

[14] P. Hu, P. H. Pathak, X. Feng, H. Fu, and P. Mohapatra, "Colorbars: increasing data rate of led-to-camera communication using color shift keying," in *Proceedings of the ACM Conference on Emerging Networking Experiments and Technologies, CoNEXT*, 2015.

[15] H. Lee, H. Lin, Y. Wei, H. Wu, H. Tsai, and K. C. Lin, "Rollinglight: Enabling line-of-sight light-to-camera communications," in *Proceedings of the Annual International Conference on Mobile Systems, Applications, and Services, MobiSys*, 2015.

[16] Y. Yang and J. Luo, "Boosting the throughput of led-camera VLC via composite light emission," in *Proceedings of the IEEE Conference on Computer Communications, INFOCOM*, 2018.

[17] Y. Yang, J. Nie, and J. Luo, "Reflexcode: Coding with superposed reflection light for led-camera communication," in *Proceedings of the Annual International Conference on Mobile Computing and Networking, MobiCom*, 2017.

[18] S. Schmid, L. Arquint, and T. R. Gross, "Using smartphones as continuous receivers in a visible light communication system," in *Proceedings of the ACM Workshop on Visible Light Communication Systems, VLCS@MobiCom*, 2016.

[19] Z. Yang, Z. Wang, J. Zhang, C. Huang, and Q. Zhang, "Wearables can afford: Light-weight indoor positioning with visible light," in *Proceedings of the Annual International Conference on Mobile Systems, Applications, and Services, MobiSys*, 2015.

[20] C. Chan, H. Tsai, and K. C. Lin, "POLI: long-range visible light communications using polarized light intensity modulation," in *Proceedings of the Annual International Conference on Mobile Systems, Applications, and Services, MobiSys*, 2017.

[21] S. D. Perli, N. Ahmed, and D. Katabi, "Pixnet: interference-free wireless links using lcd-camera pairs," in *Proceedings of the ACM Annual International Conference on Mobile Computing and Networking, MobiCom*, 2010.

[22] A. Ashok, S. Jain, M. Gruteser, N. B. Mandayam, W. Yuan, and K. J. Dana, "Capacity of pervasive camera based communication under perspective distortions," in *Proceedings of the IEEE International Conference on Pervasive Computing and Communications, PerCom*, 2014.

[23] T. Falas and H. Kashani, "Two-dimensional bar-code decoding with camera-equipped mobile phones," in *Proceedings of the IEEE Annual International Conference on Pervasive Computing and Communications Workshops, PerComW*, 2007.

[24] A. Wang, S. Ma, C. Hu, J. Huai, C. Peng, and G. Shen, "Enhancing reliability to boost the throughput over screen-camera links," in *Proceedings of the ACM Annual International Conference on Mobile Computing and Networking, MobiCom*, 2014.

[25] W. Hu, H. Gu, and Q. Pu, "Lightsync: unsynchronized visual communication over screen-camera links," in *Proceedings of the ACM Annual International Conference on Mobile Computing and Networking, MobiCom*, 2013.

[26] A. Le Floch, G. Ropars, J. Enoch, and V. Lakshminarayanan, "The polarization sense in human vision," *Vision Research*, vol. 50, no. 20, pp. 2048–2054, 2010.

[27] Y. Hokazono, A. Koizuka, G. Zhu, M. Suzuki, Y. Narusue, and H. Morikawa, "Iotorch: Reliable led-to-camera communication against inter-frame gaps and frame drops," *IEEE Transactions on Mobile Computing*, vol. 20, no. 2, pp. 550–564, 2021.

[28] N. Rajagopal, P. Lazik, and A. Rowe, "Visual light landmarks for mobile devices," in *Proceedings of the IEEE/ACM International Symposium on Information Processing in Sensor Networks (part of CPS Week), IPSN*, 2014.

[29] P. Hu, P. H. Pathak, H. Zhang, Z. Yang, and P. Mohapatra, "High speed led-to-camera communication using color shift keying with flicker mitigation," *IEEE Transactions on Mobile Computing*, vol. 19, no. 7, pp. 1603–1617, 2020.

[30] S. K. Ghiasi, M. A. Z. Zamalloa, and K. Langendoen, "A principled design for passive light communication," in *Proceedings of the ACM Annual International Conference on Mobile Computing and Networking, MobiCom*, 2021.

[31] Y. Wu, P. Wang, K. Xu, L. Feng, and C. Xu, "Turboboosting visible light backscatter communication," in *Proceedings of the Annual conference of the ACM Special Interest Group on Data Communication on the applications, technologies, architectures, and protocols for computer communication, SIGCOMM*, 2020.

[32] J. Grubor, S. Lee, K. D. Langer, T. Koonen, and J. W. Walewski, "Wireless high-speed data transmission with phosphorescent white-light leds," in *Optical Communication-post-deadline Papers*, 2007.

[33] Samsung, "product isocell hmx," https://semiconductor.samsung.com/cn/image-sensor/mobile-image-sensor/isocell-bright-hmx, 2022.

[34] P. Adam, P. Bertolino, J. M. Chassery, and F. Lebowsky, "Lcd response time estimation," in *Proceedings of the International Display Research Conference*, 2006.

[35] J. M. Kim, S. H. Lee, D. H. Jeon, and S. W. Lee, "Physical model of pixels in twisted nematic active-matrix liquid crystal displays," *IEEE Transactions on Electron Devices*, vol. 62, no. 10, pp. 3308–3313, 2015.

[36] Wikipedia contributors, "Ycbcr — Wikipedia, the free encyclopedia," 2022.

[37] Matlab, "Regionprops," https://ww2.mathworks.cn/help/images/ref/regionprops.html, 2022.

[38] MATLAB, "Perspective control," https://www.mathworks.com/matlabcentral/fileexchange/35531-perspective-control-correction, 2022.

[39] A. Rosebrock, "Perspective transform," https://pyimagesearch.com/2014/08/25/4-point-opencv-getperspective-transform-example/, 2014.

[40] MATLAB, "bwboundaries," https://ww2.mathworks.cn/help/images/ref/bwboundaries.html, 2022.

[41] Y. Yang, J. Luo, C. Chen, W. Zhong, and L. Chen, "Synlight: Synthetic light emission for fast transmission in COTS device-enabled VLC," in *Proceedings of the IEEE Conference on Computer Communications, INFOCOM*, 2019.

[42] N. Cen, N. Dave, E. Demirors, Z. Guan, and T. Melodia, "Libeam: Throughput-optimal cooperative beamforming for indoor visible

light networks," in *Proceedings of the IEEE Conference on Computer Communications, INFOCOM*, 2019.
[43] A. Duque, R. Stanica, H. Rivano, and A. Desportes, "Unleashing the power of led-to-camera communications for iot devices," in *Proceedings of the ACM Workshop on Visible Light Communication Systems, VLCS@MobiCom*, 2016.
[44] G. J. Blinowski, "Security of visible light communication systems - A survey," *Physical Communication*, vol. 34, pp. 246–260, 2019.
[45] M. Cui, Y. Feng, Q. Wang, and J. Xiong, "Sniffing visible light communication through walls," in *Proceedings of the ACM Annual International Conference on Mobile Computing and Networking, MobiCom*, 2020.

Xiang Zou received the BS degree from Xi'an University of Posts and Telecommunications in 2014. He received the Master degree from Chang'an University in 2018. He is working toward the Ph.D. degree at Xi'an Jiaotong University. He research interests include RFID, VLC, mobile computing, and smart sensing.

Jianwei Liu received the BS degree from Northwestern Polytechnical University in 2018. He received his Master degree from Xi'an Jiaotong University in 2021. He is working toward the Ph.D. degree at Zhejiang University. His research interests include RFID, mobile computing, and smart sensing.

Jinsong Han received his Ph.D. degree from Hong Kong University of Science and Technology in 2007. He is currently a professor of the School of Cyber Science and Technology, Zhejiang University. His research interests focus on IoT security, smart sensing, wireless and mobile computing.

Zhi Wang received his Ph.D. degree in Computer Science from Xi'an Jiaotong University in 2014. His research interests focus on wireless networks, smart sensing, and mobile computing.